

Soft-glass model for the relaxation kinetics of red blood cells

Author: Raúl Mañas Fernández

Facultat de Física, Universitat de Barcelona, Diagonal 645, 08028 Barcelona, Spain.

Advisors: Marta Gironella-Torrent and Felix Ritort

Small Biosystems Lab, Departament de Física de la Matèria Condensada,

Facultat de Física, Universitat de Barcelona, 08028 Barcelona, Spain

Abstract: We use a soft-glass mechanical (SGM) model to reproduce the experimental force relaxation curves of red blood cells (RBC) measured by laser optical tweezers (LOT). The relaxation experiments consist in applying a deformation step jump and observe how the force, after reaching a maximum, decreases with time. The SGM model has been already successful to reproduce the LOT experimental pulling cycles of erythrocytes. We extend our model to reproduce the experimental relaxation curves if nicely predicts the stationary force of the relaxation in terms of the maximum force achieved immediately after the extension step-jump.

I. INTRODUCTION

Red blood cells (RBC) or erythrocytes are the most common type of blood cell and vertebrate's principal mean of delivering oxygen to the body tissues via the circulatory system. In humans, 2.4 million RBC are produced per second. RBC are flexible and oval biconcave disks that lack of nucleus and organelles. In this way RBC maximize the room for hemoglobin which resides in the cytosol. RBC have a bipidic layer composed by carbohydrates and proteins, mainly spectrin and actin.

In their path through the human body, RBC suffer all kinds of deformation, even entering on the capillary network. Capillars have a smaller radius than the cell itself (3 μ m vs 6 μ m). When a external force is applied to a material, the internal forces of the body act in opposite direction to the applied force. Due to mechanical stress, the body is deformed, changing its shape. After the deformation, RBC recover the original shape, but it is uncertain if the internal properties remain constant. It is reasonable to expect that the RBC is damaged in some way, leading to its aging, and further replacement by new RBCs with mechanical properties intact.

For this reason, it is very important to study the dynamics of the RBC's mechanical properties, in other words, how they evolve in time. In order to do so, very different techniques have been used, from high output setups as magnetic tweezers [1] or Acoustic Force Spectroscopy [2], to single cell devices as LOT [3, 4].

In this work, we use a two state model, successfully used to reproduce DNA condensation in the presence of dendrimers [5] and RBC pulling experiments Fig. 1 [6], in order to simulate the experimental force-relaxations curves of RBC obtained by optical tweezers.

II. RELAXATION EXPERIMENTS

One of the most useful techniques to study molecular and cellular systems, such as RBC, are LOT. Our experimental setup consists of two counterpropagating lasers

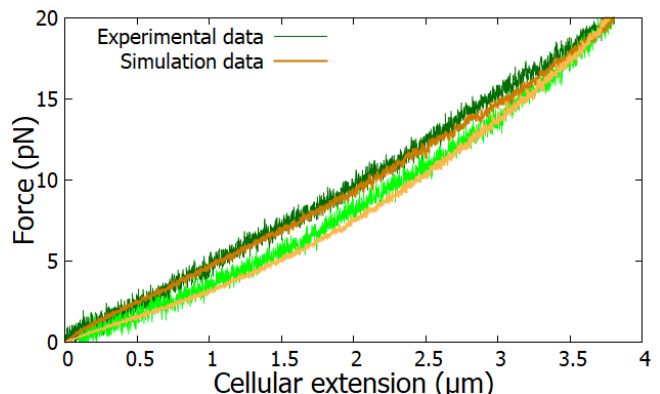


FIG. 1: Experimental pulling cycle compared with the two state model simulation. A pulling cycle consists in stretching (dark green) the RBC from a minimum force (0 pN) to a maximum force (20 pN) at constant velocity. When the system reaches the maximum force, the RBC is pushed (light green) backwards with the same velocity value until the minimum force is reached.

beams that are focused on a spot, to form the optical trap. Both lasers create an electrical field gradient, being stronger in the middle of the beam and weaker on the sides. The dielectric particles, such as polyesterine beads, are trapped in the highest electric field region [7]. Once an object is optically trapped, forces and displacements can be exerted by moving the optical trap in both horizontal and vertical axis.

The optical trap is given by the harmonic potential as

$$V(x_b) = \frac{1}{2}k_b x_b^2 \quad (1)$$

where k_b is the trap stiffness and x_b is the distance of the trapped bead and the center of the trap.

Once k_b is calibrated, we convert the measured force, f , into the bead position, x_b ,

$$f(x_b) = k_b x_b \quad (2)$$

The experimental configuration to exert force to a RBC in the vertical direction is shown in Fig. 2 (a). Two beads

are symmetrically attached to the opposites sides of the RBC. The lower bead is fixed by air suction to the tip of a micropipette, and the upper one is optically trapped.

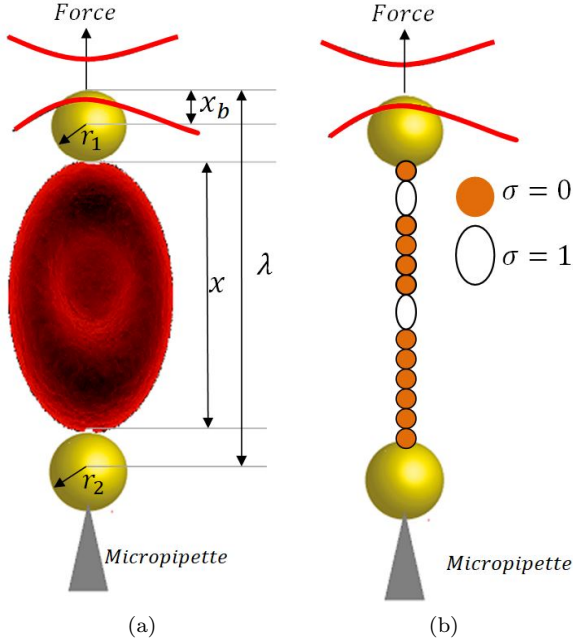


FIG. 2: a) Schematics of the system and its characteristic distances. The radius of the beads (yellow spheres) are expressed as r_1 and r_2 , x is the RBC extension, x_b is the optical trap extension and λ is the distance between the center of the lower bead and the center of the optical trap (represented with red lines). b) Schematics of the RBC modelling as an unidimensional chain formed by formed (orange spheres) and disrupted blobs (empty ellipses).

The relaxation experiments consist in applying a step function to trap position, λ . This is given by

$$\lambda = r_1 + r_2 + x + x_b \quad (3)$$

where r_1 and r_2 are the radius of the upper and lower beads respectively (notice that $r_1 = r_2 = r$) and x is the cell extension.

For a positive $\Delta\lambda$, the force immediately increases to a maximum value and then decreases until it reaches a stationary force Fig. 3. The force relaxation is measured during 150s after the deformation step jump. Notice that as r_1 and r_2 are constants, the variation of λ will only depend on x_b and x .

$$\Delta\lambda = \Delta x + \Delta x_b \quad (4)$$

III. TWO STATE MODEL FOR RBC RELAXATION CURVES

In order to reproduce the force relaxation curve, we model the RBC as an unidimensional chain formed by

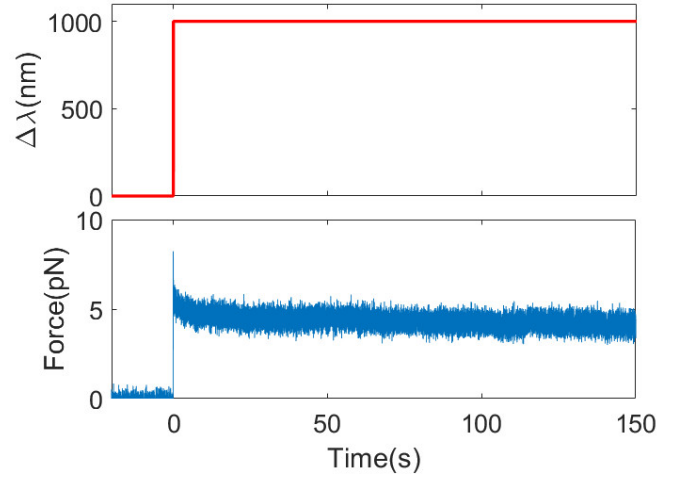


FIG. 3: $\Delta\lambda$ and force respect to time for an experimental relaxation curve. While the controlled parameter λ performed a step function, the force respond reaching a maximum at $t=0s$ and decreasing its value until a stationary state after 150s.

N blobs where each blob can be in two different states: formed if $\sigma = 0$ or disrupted if $\sigma = 1$. The free energy landscape that represents the two state model that characterized each blob is shown in Fig. 4. In order to pass from one state to the other, the blob has to overcome an energetic barrier b_i which is placed at a distance x_i from the closed state. The two states, represented by two wells, have an energy difference of Δg_i and are separated by a distance of x_m .

Both characteristic energies Δg_i and b_i depend on the force applied to the system as follows,

$$b_i(f) = b_{i0} - f x_i \quad (5)$$

$$\Delta g_i(f) = \Delta g_{i0} - f x_m \quad (6)$$

The kinetic rates, that characterize the transition between the closed(0) and opened(1) states, can be expressed as,

$$k_{0 \rightarrow 1} = k_m e^{-b_i(f)/k_B T} \quad (7)$$

$$k_{1 \rightarrow 0} = k_m e^{-(b_i(f) + \Delta g_i(f))/k_B T} \quad (8)$$

In order to simulate the experimental data Fig. 3, we impose that all the blobs are at $\sigma = 0$ at $t = 0s$ and apply $\Delta\lambda = 1000nm$. Initially, $\Delta\lambda$ leads to an irreversible jump Δx_{b0} , so the force will be $f_0 = k_b \Delta x_{b0}$. Subsequently after, $\Delta\lambda$ remains constant but will be distributed between Δx_b and Δx as shown in Eq. (4). From f_0 , the initial energy distributions $f(b_{i0})$ and $f(\Delta g_{i0})$ will be modified according to Eq. (5,6).

At every time step ($dt = 0.01s$), we sequentially and randomly select $N=1000$ blobs of the blob chain. To update each blob according to Eq. (7,8) we compare the

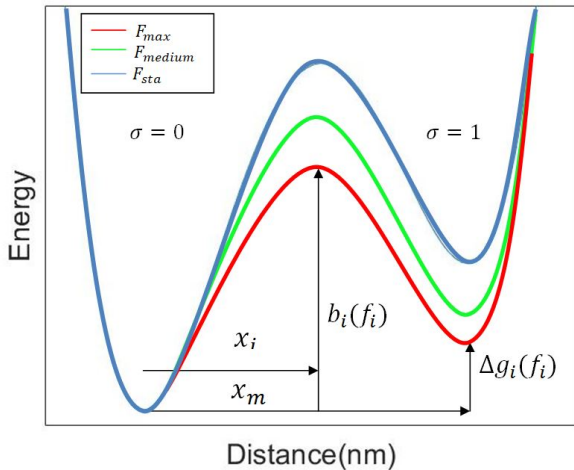


FIG. 4: Qualitative free energy landscape of the two state model. It presents two minima corresponding to the opened and closed states and a unstable one between them characterized by a barrier b_i . The red line is the free energy landscape at a maximum force, F_{max} , the moment immediately after the $\Delta\lambda$ jump, the green line represents the landscape at an intermediate force, F_{medium} during the force decay and the blue line represents the minimum force, F_{sta} , when the system reaches the stationary state after 150s relaxation. As force decreases (red-green-blue), both b_i and Δg_i increase their values according to Eq. (5,6).

probability, obtained by multiplying the appropriate kinetic rate by the time step dt , to a random number that is uniformly distributed between 0 and 1. If the probability is larger than the random number, the transition to the other state will be accepted. If the selected blob is at $\sigma = 0$, we will use the kinetic rate shown in Eq. (7), while if the blob is at $\sigma = 1$ we will use the kinetic rate of Eq. (8). This is a type of Monte Carlo (MC) simulation and to map the simulation time with the real time one must compare the real time unit dt with one MC sweep. The latter is equal to N random sequentially MC steps, with one step being the updating of one individual blob.

It is interesting to analyze some cases. If the temperature increases, the thermal energy represented by $k_B T$ also does, and the kinetic rates decrease. Consequently, both probabilities will increase their value making easier to overcome the barrier b_i from both states. On the other hand, an increase of b_i , leads to a decrease of both probabilities. An increase of Δg_{i0} compensates such a decrease but only on the closing probability ($1 \rightarrow 0$).

Every time a blob goes from the closed state to the opened one, it releases a certain amount of extension x_m to the total length of the RBC, represented by L_c , the counter length. On the reverse process, when a blob is opened and a transition to the closed state is accepted, L_c will decrease by x_m .

The model used to calibrate the extension of the RBC, when a certain force is measured, is the worm-like

chain(WLC),

$$f = \frac{k_B T}{p} \left[\frac{1}{4(1-x/L_c)^2} - \frac{1}{4} + \frac{x}{L_c} \right] \quad (9)$$

where k_B is the Boltzmann constant, T is the temperature, so $k_B T = 4.11 p N n m$ in our case as the experiments were performed at room temperature $298 K$. p is the persistence length, which quantifies of the bending stiffness of the RBC and L_c is the contour length which is the maximum extension of the object, in terms of our two state model. We can express it as,

$$L_c = \sum_{i=1}^N \sigma(i) x_m(i) \quad (10)$$

After 150s (15000 sweeps and $1.5 \cdot 10^7$ steps) the simulation stops.

IV. RESULTS

First we verify if the initial distance and energy distributions that are able to reproduce successfully the experimental pulling curves of RBC, also reproduce the force relaxation curves. In order to do so, we compare the experimental data from Fig. 3 with the output of our relaxation simulation starting from the initial b_i and Δg_i distributions. The result is the red line shown in Fig. 5 (a,b). Although the red line does not fit properly the experimental data, it reproduces the general trend of data.

In particular, we want to shift to higher forces the relaxation using the energy distributions. In the WLC model the force increases with the ratio $\frac{x}{L_c}$ Eq. (9). Therefore, if we want to increase the force we have to reduce L_c . As is shown in Eq. (10), L_c can be reduced by decreasing the system magnetization $\sum \sigma_i$ or by decreasing the value of x_{mi} . In order to not modify the distances reported at [6], we will decrease the system magnetization reducing the number of disrupted blobs. In energy terms, this translates in an increasing of b_i to decrease the probability to go from closed to opened state, and also an increasing of the free energy difference Δg_i in order to facilitate the opened to closed transition.

The green line presented in Fig. 5(a,b) is the result of increasing the initial energies b_i and Δg_i as shown in Fig. 5(c,d). The rest of the parameters as distances x_i , x_m and p remain unchanged.

In Fig. 5(a), in blue lines, we present an experimental force relaxation trace with its characteristic forces. The maximum force F_{max} is the Δf value that corresponds to the displacement $\Delta\lambda$, and the stationary force, F_{sta} , is the force that the system reaches after 150s relaxation.

Experimentally, it has been observed a linear relation between F_{max} and F_{sta} (blue dots and line of Fig. 5(e) characterized by,

$$F_{sta,exp} = (0.56 \pm 0.02) F_{max,exp} \quad (11)$$

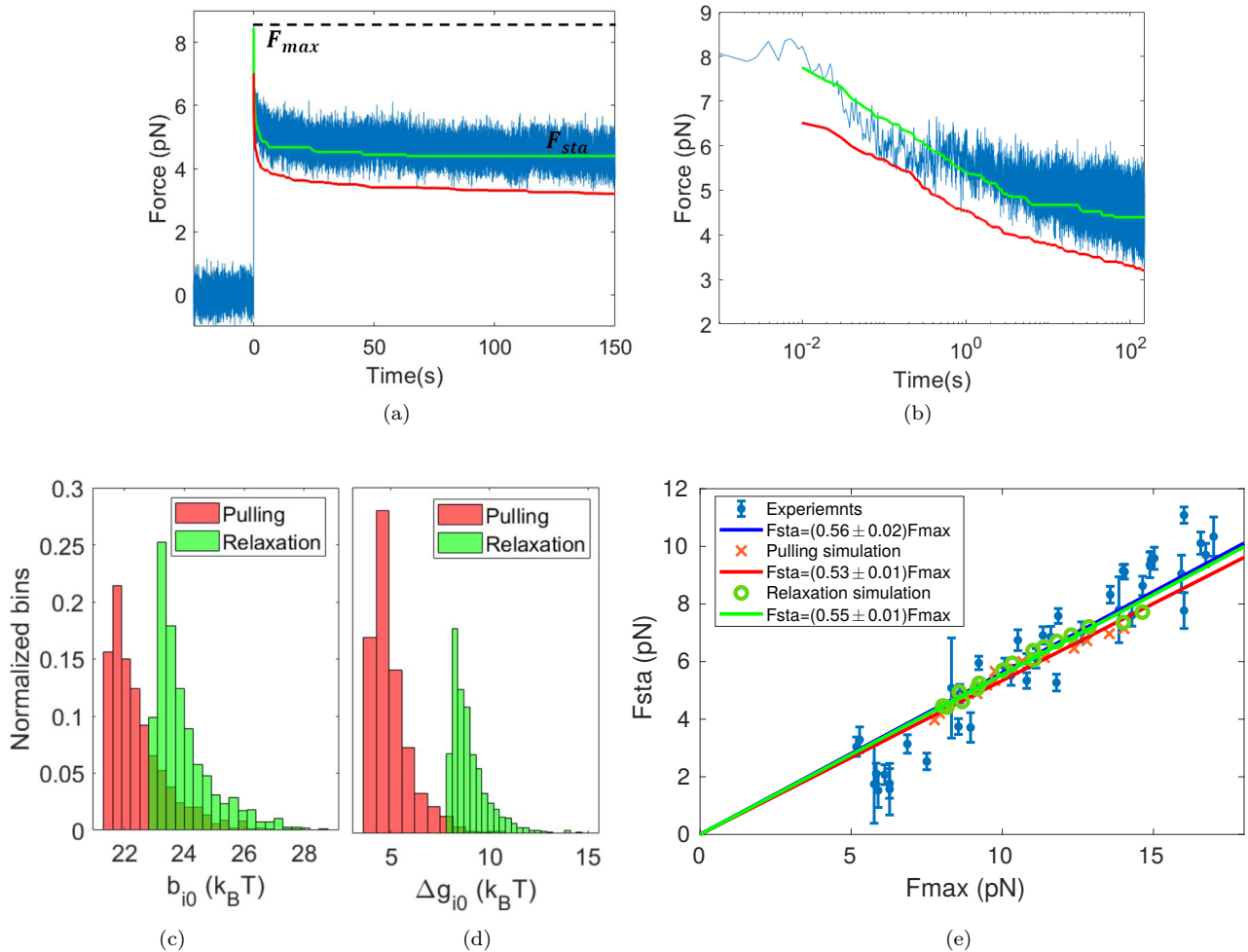


FIG. 5: a) Experimental force relaxation curve (blue) compared with simulation starting from initial energy distributions that reproduce pulling experiments (red line and red histogram at Fig. 5(c,d)). Simulation fits the experimental data by changing the initial energy distributions (green line and green histogram at Fig. 5(c,d)). F_{max} represents the maximum force reached after $\Delta\lambda$ and F_{sta} the stationary force reached after 150s. b) Experimental force relaxation curve compared with simulations in normal-log scale in order to appreciate the behaviour at short times. c) Normalized histograms of the initial b_{i0} exponential distribution used for pulling experiments (red) and force relaxation curves (green). d) Normalized histograms of initial Δg_{i0} exponential distributions used for pulling experiments (red) and force relaxation curves (green). e) Stationary force plotted versus the maximum force. Experimental data and corresponding linear regression in blue, and simulated data with corresponding pulling energies in red and its linear regression in red, and simulated data with corresponding relaxation energies in green and its linear regression in green.

For that reason, we will perform simulations for different $\Delta\lambda$ in order to verify if our model also reproduces this experimental result. In our model, each $\Delta\lambda$ yields a different relaxation curve with a pair of values F_{max} and F_{sta} . The simulation results for 15 different $\Delta\lambda$ are shown in Fig. 5(e) (green dots), and also presents a linear relation between F_{max} and F_{sta} expressed as,

$$F_{sta,sim1} = (0.55 \pm 0.01)F_{max,sim1} \quad (12)$$

If we repeat this process for the energies used for pulling experiments, we obtain the following linear relation,

$$F_{sta,sim2} = (0.53 \pm 0.01)F_{max,sim2} \quad (13)$$

V. CONCLUSIONS

- We have shown that the two state model is a valid method to reproduce experimental force relaxation curves using optical tweezers.
- The worm-like chain (WLC) is an accurate model for the force generated by the RBC and therefore

to describe the stress decay on the system after a strain deformation.

- Exponential distributions for b_i and Δg_i properly reproduce the experimental data. However, small deviations of these distributions can substantially change the relaxation curves.
- The linear relation between the simulated pair of values F_{sta} and F_{max} is in very good agreement with the experimental results for both pulling and

relaxation energy distributions.

Acknowledgments

I want to express my heartfelt gratitude to Marta, for her priceless and excellent guidance throughout the work. Also thanks to Felix Ritort for giving me the opportunity to contribute to the world of biophysics.

-
- [1] Gosse, C., Croquette, V. (2002). Magnetic tweezers: micromanipulation and force measurement at the molecular level. *Biophysical journal*, 82(6), 3314-3329.
- [2] Sorkin, R., Bergamaschi, G., Kamsma, D., Brand, G., Dekel, E., Ofir-Birin, Y., ... Wuite, G. J. (2018). Probing cellular mechanics with acoustic force spectroscopy. *Molecular biology of the cell*, 29(16), 2005-2011.
- [3] Yoon, Y. Z., Kotar, J., Yoon, G., Cicuta, P. (2008). The nonlinear mechanical response of the red blood cell. *Physical biology*, 5(3), 036007.
- [4] Zhu, R., Avsievich, T., Popov, A., Meglinski, I. (2020). Optical tweezers in studies of red blood cells. *Cells*, 9(3), 545.
- [5] Ritort, F., Mihardja, S., Smith, S. B., Bustamante, C. (2006). Condensation transition in DNA-polyaminoamide dendrimer fibers studied using optical tweezers. *Physical review letters*, 96(11), 118301.
- [6] Martin Osta, J. (2020). Simulated pulling experiments of an RNA hairpin.
- [7] SMITH, Steven B.; CUI, Yujia; BUSTAMANTE, Carlos. [7] optical-trap force transducer that operates by direct measurement of light momentum. *Methods in enzymology*, 2003, vol. 361, p. 134-162.